Available online at www.sciencedirect.com

ScienceDirect

Procedia Structural Integrity 5 (2017) 769–776

Structural Integrity Procedia

www.elsevier.com/locate/procedia

2nd International Conference on Structural Integrity, ICSI 2017, 4-7 September 2017, Funchal, Madeira, Portugal

Crack path predictions in fiber reinforced composites

Paul Judt[a]*, Jan-Christoph Zarges[b], Andreas Ricoeur[a], Hans-Peter Heim[b]

[a]*Institute of Mechanics, University of Kassel, Mönchebergstraße 7, 34125 Kassel, Germany*
[a]*Institute of Material Engineering, University of Kassel, Mönchebergstraße 3, 34125 Kassel, Germany*

Abstract

Composite materials exhibit beneficial features compared to conventional engineering material, e.g. a comparable strength and a reduced weight at the same time. To fully exploit these beneficial properties within technical structures, fracture mechanical concepts must be taken into account. The global fracture behavior in composite materials is related to the local delamination at interfaces between matrix and inclusion as well as the local fracture behaviors of the constituents. Because of their structure, the global elastic and fracture mechanical properties of composites are in general anisotropic. In this work, the directional crack resistance of polypropylene (PP) containing a certain amount of glass fibers (GF) or regenerated cellulose fibers (RCF) is measured. A crack deflection criterion based on the J-integral vector is introduced and implemented into a crack growth model. The *J*-integral is applied to calculate crack tip loading quantities on a global level, excluding all numerically inaccurate values at the crack tip. With this approach crack paths in anisotropic aluminum alloys have recently been precisely predicted. Crack growth simulations at compact tension (CT)-specimens of PP with GF and RCF are carried out, showing good agreement with the experiments. Several effects resulting from the directional crack resistance are investigated and explained, e.g. a crack deflection at mode-I loaded specimens.

Peer-review under responsibility of the Scientific Committee of ICSI 2017

Keywords: short fiber reinforced composites; crack paths; mixed-mode; anisotropy; J-integral

* Corresponding author. Tel.: +49-561-804-2852; fax: +49-451-804-2720.
E-mail address: judt@uni-kassel.de

2452-3216
Peer-review under responsibility of the Scientific Committee of ICSI 2017
10.1016/j.prostr.2017.07.168

1. Introduction

In the past, crack paths in composite materials such as in laminates, particle or fiber reinforced composites were studied e.g. by Keck and Fulland (2016), Borstnar et. al. (2016), Patrício and Mattheij (2010), Tilbrook et. al. (2005) and Wulf et. al. (1996). The difficulty of predicting the crack paths in such materials is related to the interplay of different energy consuming processes during fracture. On the one hand, the potential energy is reduced due to crack growth in the constituents of the composite. On the other, the delamination of interfaces between matrix and particles plays a crucial role with respect to the global energy release rate and the evolution of matrix cracks.

Typically, the theory of linear elastic fracture mechanics (LEFM) is adapted to formulate the crack tip stress and displacement fields and the crack tip loading quantities in a crack growth simulation. In the case of composite materials, non-linear effects of interface delamination provide an elastic-plastic material behavior on the global level and thus theoretically must be considered in the simulation. Adding a coupling agent to the bulk material leads to an embrittlement of the composite and therefore small scale yielding (SSY) conditions can be assumed.

Under SSY conditions the loading quantities of LEFM, such as stress intensity factors (SIF), energy release rate (ERR) or the *J*-integral (Rice, 1968) provide valid measures for the crack driving force or the crack deflection angle. In the following, FE-simulations in connection with a remeshing procedure with intelligent mesh refinement at the crack is applied to model crack growth. The crack driving force is calculated from the J_k-integral in connection with some special numerical treatment in the vicinity of the crack tip, where the numerical data are inaccurate (Judt and Ricoeur, 2013). Applying this approach to cracks in aluminum alloy specimens with anisotropic fracture toughness provides numerical crack paths that are in very good agreement with experiments (Judt et. al., 2015a).

To accurately predict the paths, details about the fracture toughness anisotropy are necessary, which are obtained from e.g. CT-tests. In aluminum alloys the fracture toughness anisotropy is related to the texture of the microstructure. Zarges et. al. (2017) and Judt et. al. (2017) investigated the anisotropy of the crack resistance in short fiber reinforced PP composites, which are related to the orientation of the crack ligament with respect to the predominant fiber orientation. The authors investigated crack paths in initially mode-I loaded CT-specimens with different predominant directions and observed an immediate crack deflection in certain specimen configurations. This phenomenon was also observed by Keck and Fulland (2016) and is related to the fracture toughness anisotropy.

In this paper the effects of a small plastic zone in front of the crack tip are investigated, regarding the absolute value of the loading quantity and the crack deflection angle. Furthermore, the experimental crack paths in composites with a coupling agent are compared to calculated paths.

Nomenclature

a	crack length
A	surface
b	specimen thickness
d_p	expansion of the plastic zone along the ligament
G	energy release rate
J_c	crack resistance
J_c^{PD}	crack resistance for crack growth parallel to the predominant direction
J_c^{TD}	crack resistance for crack growth transverse to the predominant direction
J_k	*J*-integral vector
K_I	mode-I stress intensity factor
K_II	mode-II stress intensity factor
n_j	normal vector
Q_{kj}	energy-momentum tensor
R	radius of a circular integration contour Γ_0
t	expansion of the plastic wake perpendicular to the crack faces
u	strain energy density
u^e	contribution of the elastic strains to the stress work density
u_i	displacement vector

z_k	unit vector parallel to the crack growth direction
β	ratio of the coordinates of the J_k-integral vector
γ	angle between ligament and predominant direction
δ_{ij}	Kronecker delta
ε_{ij}^{p}	plastic strain tensor
φ	polar angle
Γ_c	integration contour at crack faces
Γ_ε	infinitely small integration contour
Γ_0	finite integration contour
σ_{ij}	stress tensor
χ	ratio of the directional fracture toughness

2. Numerical investigations at small plastic zones

According to the theory of the material space, configurational forces act on defects, such as notches, interfaces, free surfaces or in general due to material inhomogeneity (Kienzler and Herrmann, 2000). Material forces appearing at cracks obtain a physical significance as they represent the ERR due to crack growth. The J_k-integral vector (Budiansky and Rice, 1973)

$$J_k = \lim_{\Gamma_\varepsilon \to 0} \int_{\Gamma_\varepsilon} Q_{kj} n_j ds = \lim_{\Gamma_\varepsilon \to 0} \int_{\Gamma_\varepsilon} \left(u\delta_{kj} - \sigma_{ij} u_{i,k} \right) n_j ds \,, \tag{1}$$

with Q_{kj} being the energy-momentum tensor, n_j the outward normal at the infinitely small contour Γ_ε, u the strain energy density, σ_{ij} the stresses and u_i the displacement vector, is equivalent to the material force at a crack tip, thus representing a measure for the crack driving force. In LEFM J_k is related to the SIF (Bergez, 1974) and the ERR (Irwin, 1958). Due to the inherent path-independence of J_k, an arbitrary integration path may be chosen for the calculation of the integral. Especially in a FE-framework, large integration contours Γ_0 are beneficial as inaccurate numerical data in the vicinity of the crack tip are excluded from the calculation. This integral provides the sum of all material forces which are surrounded by the integration contour Γ_0 and therefore additional integrals along other defects must be included to obtain path-independence and calculate the crack driving force. In the case of an elastic-plastic material behaviour an additional domain integral is necessary and considering Γ_0, Eq. (1) reads (Carpenter et. al., 1986)

$$J_k = \lim_{\Gamma_\varepsilon \to 0} \int_{\Gamma_\varepsilon} \left(u^e \delta_{kj} - \sigma_{ij} u_{i,k} \right) n_j ds = \int_{\Gamma_0} Q_{kj} n_j ds + \int_{\Gamma_0} [\![Q_{kj}]\!]^{+}_{-} n_j ds + \int_{A} \sigma_{ij} \varepsilon^{p}_{ij,k} dA, \tag{2}$$

where ε_{ij}^{p} are the plastic strain, u^e is the specific elastic potential and A the domain enclosed by Γ_0. The crack face integral along Γ_c represents the jump of the energy-momentum tensor across the crack faces. Compared to the linear-elastic case, the driving force of a crack in an elastic-plastic material is smaller due to additional energy consuming processes forming the plastic crack tip zone. Next to the crack driving force, the material behaviour may also have an effect on the crack deflection angle.

Numerical investigations of a plane model of the CT-specimen shown in Fig. 1(a) are performed. By clamping the right edge of the specimen and loading it with a vertical (mode-I) or horizontal (mode-II) displacement of the two bolts that are fitted into the holes shown in Fig. 1(b), a normal crack opening (mode-I) or in-plane crack shearing (mode-II) are obtained. In Fig. 1(b) the material forces, calculated according to Mueller et. al. (2002), are depicted at mode-I loaded specimen with elastic material. The force at the crack tip is equivalent to J_k-integral vector. In the following, the material behaviour is assumed as linear-elastic or elastic perfectly-plastic.

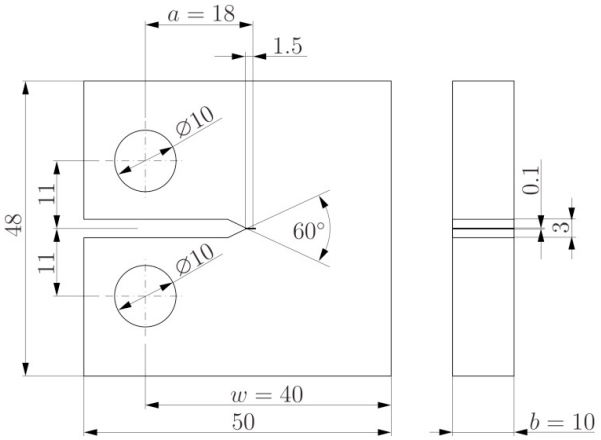

(a) Geometric dimensions of the CT-specimens

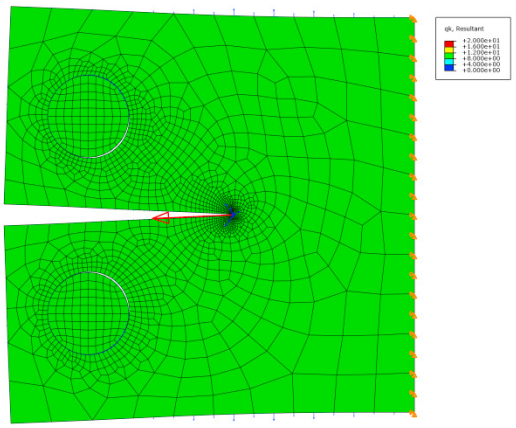

(b) Mode-I loaded CT-specimen, material forces

Fig. 1. (a) Dimensions of a CT-specimen according to ASTM D5045-99, (b) deformed CT-model under mode-I crack loading and material forces

Considering a mode-I and a mixed mode-I/II crack loading scenario, the J_k-integrals and SIF are calculated and compared in Tab. 1. In case of an elastic-plastic material the SIF, which are obtained from J_k, are no longer crack loading quantities and are thus put in parentheses.

Table 1. Path-independent J_k-integrals and SIF at CT-specimens with elastic and elastic-plastic material

Loading and material scenario	J_1 / (N/mm)	J_2 / (N/mm)	K_I / MPa$\sqrt{\text{m}}$	K_{II} / MPa$\sqrt{\text{m}}$	d_p / mm
mode-I, elastic	22.62	0.0	9.39	0.0	-
mode-I, plastic	12.85	0.0	(7.08)	(0.0)	4.61
mixed-mode, elastic	23.68	3.44	9.58	-0.70	-
mixed-mode, plastic	9.12	6.48	(5.50)	(-2.30)	4.64

The path-independence of the elastic-plastic J_k-integral is investigated by applying Eq. (2) with circular contours Γ_0 of different radii R. In Fig. 2, J_k is plotted vs. R and by considering the crack face integrals Γ_c and the domain integral in Eq. (2), the path-independence is preserved (blue line). The line integral along Γ_0 (green line) is not path-independent, as long as the contour runs through plasticised regions. By considering the domain integral (pink line), the material forces, acting e.g. in the crack tip plastic zone, are separated from the crack driving force. For comparison the J_k-integral of the linear-elastic case is also plotted (red line), showing noticeably larger values than for the elastic-plastic material.

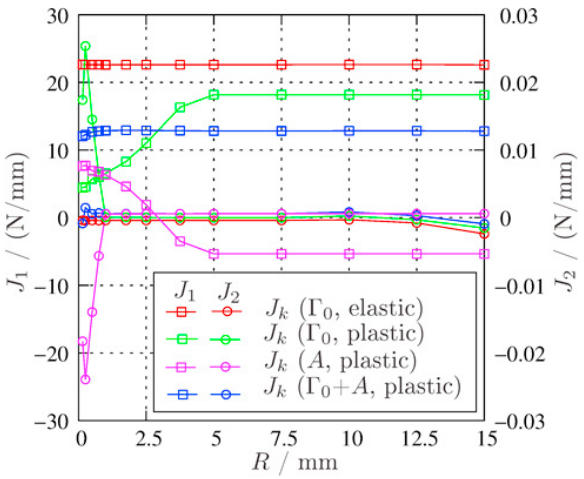

(a) mode-I crack tip loading

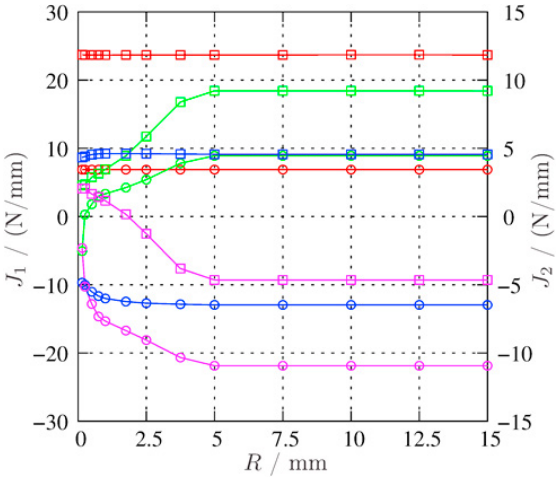

(b) mixed-mode crack tip loading

Fig. 2. Investigations of the path-independence in CT-specimens with elastic-plastic material behavior and comparison with the elastic case

Other path-independent integrals, like the M and L-integral, can be applied to provide a measure for the size of the plastic zone (Judt and Ricoeur, 2015b). The size of the expansion of the plastic zone along the ligament d_p during the calculations is depicted in Tab. 1. The crack deflection angle obtained from the J-integral vector criterion depends on the ratio of the coordinates $\beta = J_2 / J_1$. From the J_k-values in Tab. 1 it becomes obvious, that for a mixed-mode loading the ratio of the linear-elastic material behaviour is different than in the elastic-plastic case and thus provides differing crack deflection angles.

3. Specimen preparation and experiments

In experiments at CT-specimens of short GF and RCF reinforced PP composites the critical J_c-values are measured for different predominant directions (PD) and the crack paths are investigated. The CT-specimens are drilled out from plates of thickness b=10mm, which are manufactured by injection molding. To study the influence of the fiber alignment in the specimen on J_c-values and crack paths, CT-specimens of different notch orientation with respect to the melt flow direction (MFD) were prepared, see Fig. 3. The shape of CT-specimens according to Fig. 1(a) and the experimental procedures are in accordance with ASTM D5045-99.

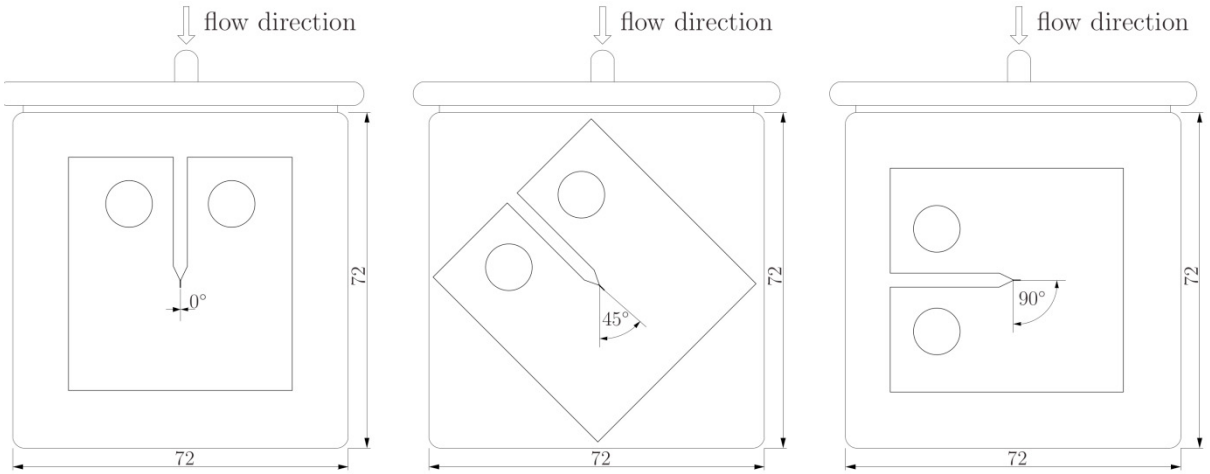

(a) Notch parallel (0°) to MFD (b) Notch diagonal (45°) to MFD (c) Notch perpendicular (90°) to MFD

Fig. 3. CT-specimen extraction from injection molded plates exhibiting different notch orientations: (a) notch parallel to MFD, transverse direction (TD), (b) notch diagonal to MFD, (c) notch perpendicular to MFD, predominant direction (PD)

During the experiments considerable plastic zones around the crack tip were observed leading to a plastic wake in the case of crack growth, see Fig. 5. To improve the fiber-matrix adhesion by increasing the interfacial shear strength, a coupling agent is added to the compound. As a result of the improved interfacial shear strength, higher loads can be transferred form the matrix polymer to the fiber. A lower fiber-matrix adhesion leads to a failure of the interface and a fiber pull-out, whereas a good adhesion leads to a fiber breakage due to reaching the tensile strength. The quality of the adhesion depends on the building of chemical bonds (covalent bonding) between fibers and matrix polymer as well as on the physical constellations, e.g. shape and dimension of the fibers.

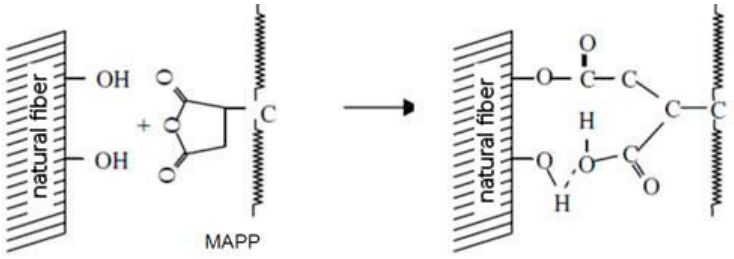

Fig. 4. Chemical improvement of fiber-matrix adhesion with the coupling agent MAPP

In case of the polypropylene, a maleic anhydride acid crafted polypropylene (MAPP) is often used as coupling agent, which has a PP backbone and functional side groups. The functional principle of the coupling agent is shown in Fig. 4. It can be seen that MAPP owns nonpolar sections and polar functional side groups which react with the hydroxyl groups of the cellulosic fibers by building covalent ester bonds. The newly created carboxyl groups (-COOH) can build hydrogen bonds with the free hydroxyl groups of the cellulosic fibers whereas the nonpolar backbone of the MAPP shows a high affinity the PP matrix. Applying this coupling agent provides an embrittlement of the composite CT-specimens and thus leads to much smaller plastic zones during crack growth.

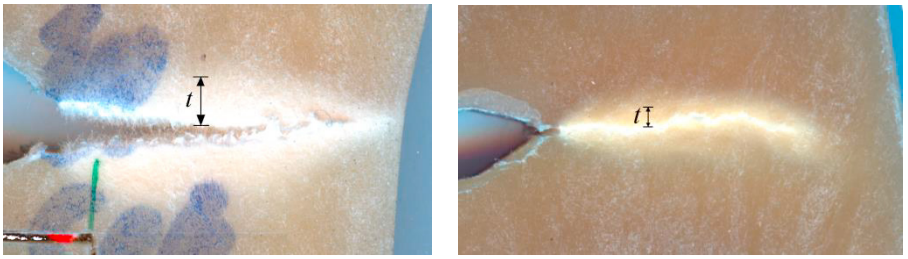

(a) Plastic wake in PP 30 wt-% RCF (t^{wo}) (b) Plastic wake in PP 30 wt-% RCF, 3 wt-% MAPP (t^{w})

Fig. 5. Comparison of the plastic wake at RCF reinforced PP composites with and without coupling agent

The plastic wake surrounding the crack is depicted in Fig. 5, comparing composites with (w) and without (wo) coupling agent. The analysis of the wake's size t reveals a reduction due to the coupling agent by $t^{w}=0.35t^{wo}$, where $t^{wo}=3.44$mm. In Tab. 2 the measured J_c-values for the different notch orientations are presented. The coupling agent provides a reduction of the J_c -values from 17% up to 27%. The specimens of PP composite with 30 wt.-% RCF and 3 wt.-% MAPP are shown in Fig. 6. The specimens differ in the alignment of the notch with respect to the MFD or the PD, respectively.

Table 2. J_c-values and standard deviation (SD) from CT-tests with different notch orientation, ratio of the orthotropic crack resistance

composite	J_c, (0°, TD)	SD	J_c, (45°)	SD	J_c, (90°, PD)	SD	$\chi=\sqrt{J_c^{TD}/J_c^{PD}}$
PP 20 wt-% RCF, 2 wt-% MAPP	29.8	3.3	17.5	0.4	13.3	3.4	1.49
PP 30 wt-% RCF, 3 wt-% MAPP	31.6	3.8	16.8	1.9	12.9	2.1	1.56
PP 30 wt-% GF, 3 wt-% MAPP	11.5	2.2	8.2	0.4	7.2	1.0	1.26

4. Crack path prediction and comparison

With the method explained in Sec. 2, crack paths are calculated in CT-specimens according to Figs. 1(a) and 3. Due to the coupling agent, the size of the plastic zone at the crack tip is considerably smaller and thus SSY conditions are assumed. The crack tip loading J_k is calculated following Eq. (2) along finite integration contours Γ_0. Because of the SSY conditions, the domain integral can be omitted. The crack deflection angle is predicted by the J-integral criterion (Strifors, 1974, Ma and Korsunsky, 2005), thus the crack grows in to the direction of the J_k-vector and maximizes the energy release rate by

$$G = J_k z_k = \sqrt{J_1^2 + J_2^2} \tag{3}$$

with z_k being the unit vector pointing in the direction of the crack extension. A modification of this criterion is necessary for the application at cracks in anisotropic materials (Judt et. al., 2015a, 2017). In these materials, the critical fracture mechanical parameter J_c is anisotropic and depends on the crack growth direction as has been shown in Sec. 3. In the model, this parameter is implemented applying an interpolation function (Kfouri, 1996)

$$J_c(\varphi) = \frac{J_c^{TD} J_c^{PD}}{J_c^{TD}\cos(\varphi+\gamma)^2 + J_c^{PD}\sin(\varphi+\gamma)^2} \tag{4}$$

with the polar angle φ and the angle between ligament and predominant direction γ. The angle γ does not coincide with the angle shown in Fig. 3. For $\gamma = 0°$ the angle is equivalent to 90° in Fig. 3 and in the case of $\gamma = 90°$ the angle of 0° in Fig. 3 holds. In the modified criterion, the crack grows into the direction where the ratio $J_R = G / J_c$ is a maximum.

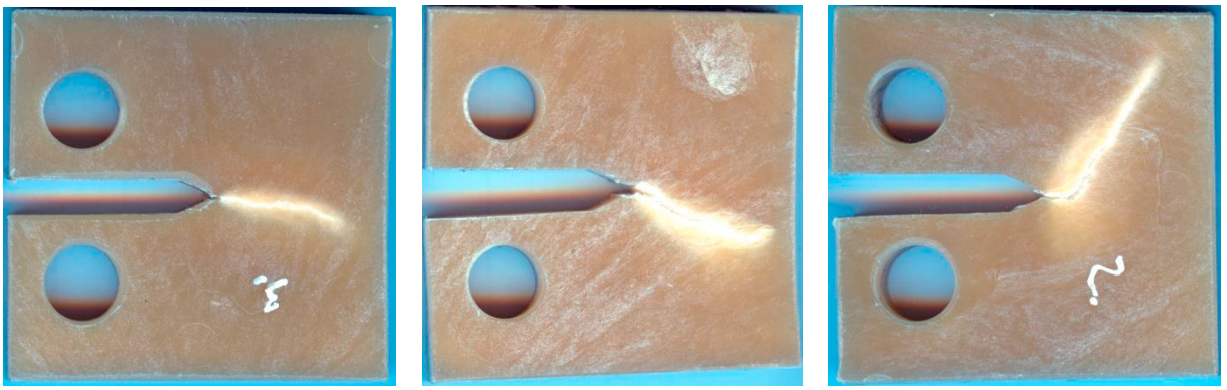

(a) $\gamma = 0°$ (b) $\gamma = 45°$ (c) $\gamma = 90°$

Fig. 6. Experimental crack paths in CT-specimens (PP with 30 wt.-% RCF and 3 wt.-% MAPP) under mode-I loading with different notch alignments γ

The resulting crack paths from simulation and experiments are depicted in Fig. 7. The simulation corresponds very well with the experiments and reproduces the crack deflection in the cases of $\gamma = 45°$ and $\gamma = 90°$ despite of the externally induced mode-I loading. This phenomenon was also observed by e.g. Keck and Fulland (2016).

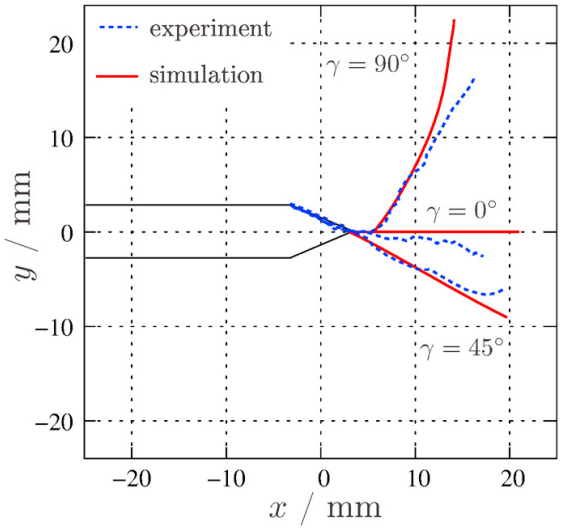

Fig. 7. Comparison of numerical and experimental crack paths in PP composites with RCF fibers and a coupling agent

4. Conclusions

The anisotropic features of composite materials are strongly related to the material's microstructure. In the case of injection molded short fiber reinforced composites, these features are related to the predominant alignment of the fibers. Their alignment follows the shape of the flow front during the casting process, thus exhibiting a spatial dependence in the anisotropy of the mechanical parameters. The application of a coupling agent provides an embrittlement of the composite, so that the size of plastic zone in front of the crack tip shrinks. Although in this investigation the spatial variance and the effects of plasticity are neglected, the calculated crack paths in CT-specimens are in good agreement with the experimental paths.

Acknowledgement

The authors would like to acknowledge the financial support of the "Landes-Offensive zur Entwicklung Wissenschaftlich-ökonomischer Exzellenz (LOEWE)" Research Funding Program "Safer Materials".

References

ASTM D5045-99, 2007. Standard test method for plane-strain fracture toughness and strain energy release rate of plastic materials. ASTM International.

Bergez D., 1974. Determination of stress intensity factors by use of path-independent integrals. Mechanics Research Communications 1, 179–180.

Borstnar G., Mavrogordato M.N., Yang Q.D., Sinclair I., Spearing S.M., 2016. Crack path simulation in a particle-toughened interlayer within a polymer composite laminate. Composites Science and Technology 133, 89-96.

Budiansky B., Rice J.R., 1973. Conservation laws and energy-release rates. Journal of Applied Mechanics 40(1), 201–203.

Carpenter W.C., Read D.T., Dodds R.H., Jr., 1986. Comparison of several path independent integrals including plasticity effects. International Journal of Fracture 31, 303–323.

Irwin G.R. 1958. Fracture in "*Encyclopedia of physics: elasticity and plasticity, Volume 6*". In: Fluegge S. (Ed.). Springer, Berlin, pp. 551–590.

Judt P.O., Ricoeur A., 2013. Accurate loading analyses of curved cracks under mixed-mode conditions applying the J-integral. International Journal of Fracture 182, 53–66.

Judt P.O., Ricoeur A., Linek G., 2015a. Crack path prediction in rolled aluminum plates with fracture toughness orthotropy and experimental validation. Engineering Fracture Mechanics 138, 33–48.

Judt P.O., Ricoeur A., 2015b. Crack path predictions and experiments in plane structures considering anisotropic properties and material interfaces. Frattura et Intigritá Strutturale 24, 208-215.

Judt P.O., Zarges J.-C., Ricoeur A., Heim H.-P., 2017. Anisotropic fracture properties and crack path prediction in glass and cellulose fiber reinforced composites. Submitted to Engineering Fracture Mechanics

Keck S., Fulland M., 2016. Effect of fibre volume fraction and fibre direction on crack paths in flax fibre-reinforced composites. Engineering Fracture Mechancis 167, 201-209.

Kfouri A.P., 1996. Crack extension under mixed-mode loading in an anisotropic mode-asymmetric material in respect of resistance to fracture. Fatigue and Fracture of Engineering Materials and Structures 19, 27–38.

Kienzler R., Herrmann G., 2000. Mechanics in material space with applications to defect and fracture mechanics. Springer, Berlin.

Ma L., Korsunsky A.M., 2005. On the use of vector J-integral in crack growth criteria for brittle solids. International Journal of Fracture 133, L39–L46.

Mueller R., Kolling S. und Gross D., 2002. On configurational forces in the context of the finite element method. International Journal for Numerical Methods in Engineering 53, 1557–1574.

Patrício M., Mattheij R.M.M., 2010. Crack paths in composite materials. Engineering Fracture Mechanics 77, 2251–2262.

Rice J.R., 1968. A path independent integral and the approximate analysis of strain concentration by notches and cracks. Journal of Applied Mechanics 35(2), 379–386.

Strifors H.C., 1974. A generalized force measure of conditions at crack tips. International Journal of Solids and Structures 10, 1389–1404.

Tilbrook M.T., Moon R.J., Hoffman M., 2005. Crack propagation in graded composites. Composites Science and Technology 65, 201–220.

Wulf J., Steinkopff T., Fischmeister H.F., 1996. FE-simulation of crack paths in the real microstructure of an Al(6061)/SiC composite. Acta Materialia 44(5), 1765-1779.

Zarges J.-C., Minkley D., Feldmann M., Heim H.-P., 2017. Fracture toughness of injection molded, man-made cellulose fiber reinforced polypropylene. Composites: Part A, 98, 147–158.